Sustainable Marine Structures
https://journals.nasspublishing.com/index.php/sms

ARTICLE

One-Line Modelling of Sediment Transport and Shoreline Evolution on a River-Dominated Coast: The Day Estuary, Vietnam

Cong Huu Vu [1], ***Xuan Hoan Le*** [2*], ***Nam Thanh Pham*** [3], ***Dinh Hoa Tran*** [4], ***Van Chinh Pham*** [5], ***Tien Ha Doan*** [1], ***Anh Tu Tran*** [6]

[1] *Key Laboratory of River and Coastal Engineering-Vietnam Academy for Water Resources (KLORCE), Chua Boc 165, Hanoi 11520, Vietnam*

[2] *Institute of Mechanics-Vietnam Academy of Science and Technology, Doi Can 264, Hanoi 11119, Vietnam*

[3] *Department of Hydrodynamics and Data Assimilation, Institute of Coastal Systems-Analysis and Modeling, Helmholtz-Zentrum Hereon, 21502 Geesthacht, Germany*

[4] *Vietnam Academy for Water Resources (VAWR)-Ministry of Agriculture and Rural Development, Tay Son 171, Hanoi 11520, Vietnam*

[5] *Center for Hydro-Meteorological Survey (HMSTS)-Vietnam Meteorological and Hydrological Administration, Phao Dai Lang 10, Hanoi 11527, Vietnam*

[6] *Institute of Science and Technology for Energy and Environment (ISTEE)-Vietnam Academy of Science and Technology, Da Nang 246, Hai Phong 180000, Vietnam*

ABSTRACT

The coastline surrounding the Day estuary in northern Vietnam, extending about 25 km, has experienced rapid shoreline accretion with average rates of approximately 100 m/year, while localized erosion occurs in several sections. Previous studies suggest that long-term shoreline evolution in this region is controlled by sediment supply from the Red River, reduced nearshore wave energy, and sediment trapping by the Hoa Binh Dam. In this study,

*CORRESPONDING AUTHOR:
Xuan Hoan Le, Institute of Mechanics-Vietnam Academy of Science and Technology, Doi Can 264, Hanoi 11119, Vietnam;
Email: lxhoan99@yahoo.com

ARTICLE INFO
Received: 9 December 2025 | Revised: 20 February 2026 | Accepted: 16 March 2026 | Published Online: 20 March 2026
DOI: https://doi.org/10.36956/sms.v8i1.2981

CITATION
Vu, C.H., Le, X.H., Pham, N.T., et al., 2026. One-Line Modelling of Sediment Transport and Shoreline Evolution on a River-Dominated Coast: The Day Estuary, Vietnam. Sustainable Marine Structures. 8(1): 238–257. DOI: https://doi.org/10.36956/sms.v8i1.2981

a numerical shoreline change model based on the one-line theory was applied to investigate large-scale accretion and erosion under the combined influence of riverine sediment supply and nearshore wave dynamics, while tidal currents and river flow were not explicitly simulated. The nearshore wave regime was simulated using a 2D wave transformation model driven by a 30-year deep-water wave dataset from the Global Ocean Wave Analysis (GOWA). The effect of the Hoa Binh Dam was represented by a 30% reduction in riverine sediment supply. The model was calibrated and validated against measured shoreline positions from 1965, 1989, and 2019, showing good agreement with observations and average relative errors of 9.2% and 12.5% during calibration and validation, respectively. Sediment budget analysis indicates that riverine input is the dominant source of shoreline accretion, while longshore sediment transport (LST) plays a secondary role, and part of the sediment is lost offshore. These results should be interpreted within the scope of the simplified one-line shoreline model, which targets large-scale, long-term shoreline evolution.

Keywords: Shoreline Modelling; Sediment Transport; Beach Evolution; Day Estuary; Red River

1. Introduction

Coastal zones provide essential natural resources, livelihoods, and socio-economic benefits for coastal communities, including fisheries, tourism, and ecosystem services [1, 2]. However, these areas are highly dynamic and vulnerable to natural and anthropogenic pressures, posing significant challenges for sustainable coastal management [3–5].

Sediment dynamics are fundamental in shaping shoreline morphology and controlling coastal evolution. Sediment transport processes govern the formation and development of beaches, tidal flats, estuaries, and deltaic coastlines, and are crucial for maintaining coastal stability under the influence of waves and currents [6]. Understanding sediment transport pathways and sediment budgets is therefore necessary for predicting shoreline change and assessing coastal vulnerability [7]. In river-dominated delta systems such as the Red River Delta, large sediment inputs from fluvial sources interact with coastal hydrodynamics to produce rapid and complex shoreline changes. The Red River system delivers substantial alluvial material to the coast through multiple estuaries, forming one of the most dynamic deltaic coastlines in the Gulf of Tonkin [8, 9].

The Red River Delta coastline extends approximately 165 km across Nam Dinh and Thai Binh provinces (present-day Ninh Binh and Hung Yen provinces). It receives an estimated annual sediment load of about 100×10^6 t delivered to the sea through seven major estuaries, including Van Uc, Thai Binh, Diem Dien, Tra Ly, Ba Lat, Lach Giang, and Day [10, 11]. Many of these estuaries exhibit rapid accretion rates ranging from 15 to 100 m/year [10, 11]. The present study focuses on a 25 km-long coastal segment encompassing the Day, Lach Truong, and Lach Can estuaries (**Figure 1a**), where shoreline evolution is governed by complex interactions among riverine sediment supply, waves from the Gulf of Tonkin, and coastal currents [9, 12, 13]. Long-term remote sensing analysis (1965–2023) indicates persistent shoreline accretion toward the sea, with average rates reaching about 100 m/year, and exceptionally high shoreline variability near the Day estuary [11, 12, 14]. While the abundant sediment supply from the river system is considered a primary driver of rapid accretion, the spatial distribution and temporal variability of shoreline change are strongly influenced by coastal hydrodynamic processes [12, 14, 15]. Under ongoing climate change, coastal communities may face increasing risks associated with altered sediment supply, sea-level rise, and changes in wave climate [3–5].

Previous studies in the area have primarily focused on detecting shoreline changes and predicting future trends using satellite imagery [17–19] or on estimating longshore sediment transport (LST) using simplified empirical formulations, such as the Coastal Engineering Research Center (CERC) formula [20]. However, the relative contributions of different sediment sources, including riverine inputs, LST from adjacent coastal segments, and sediment losses to deeper waters, as well as their com-

bined roles in shaping long-term shoreline morphology, remain insufficiently quantified. Therefore, this study aims to assess the relative roles of riverine sediment supply and nearshore wave dynamics in controlling shoreline accretion and sediment redistribution along the coast. A numerical shoreline change model based on one-line theory [16] is applied to quantify LST and shoreline evolution under the combined influence of sediment inputs from river systems and coastal hydrodynamics. The model is calibrated and validated using historical shoreline positions from 1965, 1989, and 2019, providing an assessment of sediment transport pathways and long-term shoreline evolution in this rapidly changing coastal system.

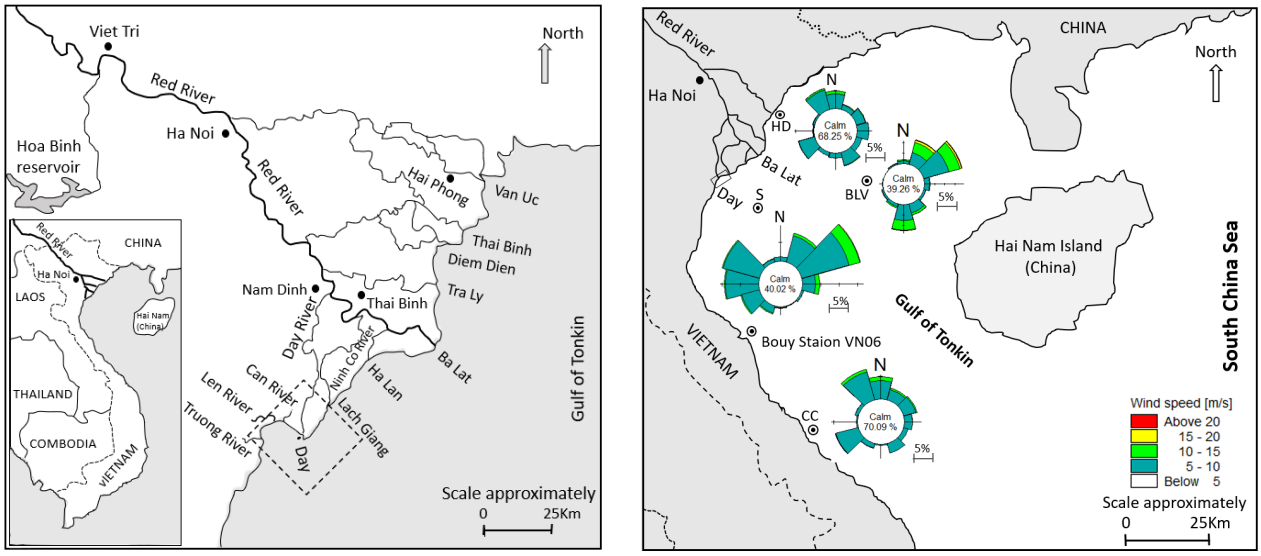

(a) **(b)**

Figure 1. (**a**) Study site and distribution of estuaries in the Red River system; (**b**) wind roses at stations surrounding the study site, based on an 18-year time series (2005–2023) with four records per day, converted to a reference height of 10 m above mean sea level.

Source: Base maps and station locations are adapted from Hoan et al. cite16.

2. Environmental and Forcing Conditions in the Study Area

2.1. Winds

The wind regime in northern Vietnam is dominated by a pronounced monsoonal system, consisting of a winter monsoon and a summer monsoon [8, 21]. During the winter monsoon, from November to March, strong northerly and northeasterly winds prevail, and are associated with relatively low air temperatures and reduced precipitation. In contrast, the summer monsoon, occurring mainly between May and September, is characterized by moderate southerly winds accompanied by higher temperatures and increased rainfall. Transitional periods between the two monsoon seasons, generally in April and October, are marked by weaker winds, often from the east, and milder weather conditions [8].

Wind rose analyses from four meteorological stations surrounding the study area (**Figure 1b**) indicate that the wind field over the Gulf of Tonkin is strongly influenced by regional topography. Among these stations, Bach Long Vi (BLV), located offshore on Bach Long Vi Island near the center of the Gulf and distant from the mainland, provides wind observations that are considered the most representative of the regional wind conditions over the Gulf of Tonkin [8].

2.2. Nearshore Topography

The nearshore zone adjacent to the Day estuary is characterized by a gently sloping seabed, creating an extensive area over which wave transformation and energy dissipation can occur [9, 14, 15]. Bathymetric data derived from a Vietnamese Navy chart, with depth corrections applied for conditions around 1980, indicate that depth

contours in the northern area of the Day estuary are generally oriented parallel to the shoreline and that the offshore seabed slope remains relatively uniform. In contrast, the southern area exhibits a gentler slope and more irregular seabed features, which enhance wave energy dissipation (**Figure 2**).

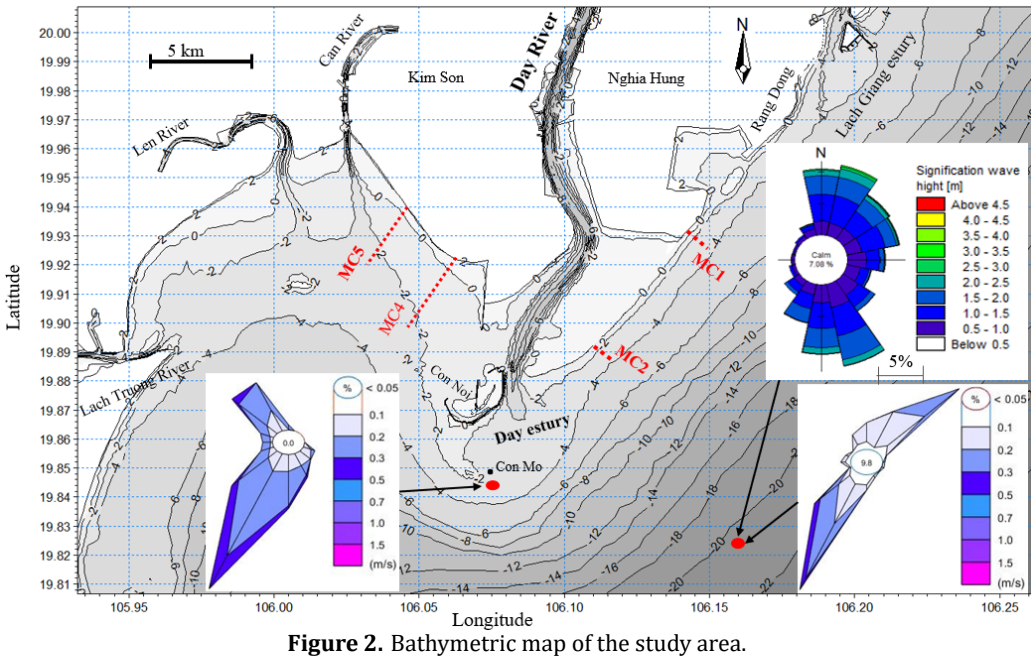

Figure 2. Bathymetric map of the study area.

Note: MC1–MC5 indicate the locations of the measured cross-shore profiles. The offshore wave rose (upper right) is based on 30 years (1993–2023) of wave reanalysis data from GOWA, and the two current prisms are derived from short-term measurements collected in 2023 at two anchored stations (indicated by red dots).

To further characterize nearshore profile morphology, four measured cross-shore profiles (MC1, MC2, MC4, and MC5; see **Figure 3**) were fitted to the equilibrium beach profile (EBP) formulation proposed by Dean [22] using a least-squares approach. The resulting values of the profile scale parameter (A) range from 0.012 to 0.041 $m^{1/3}$, corresponding to median grain sizes (D_{50}) of approximately 0.09–0.13 mm (**Table 1**) [23].

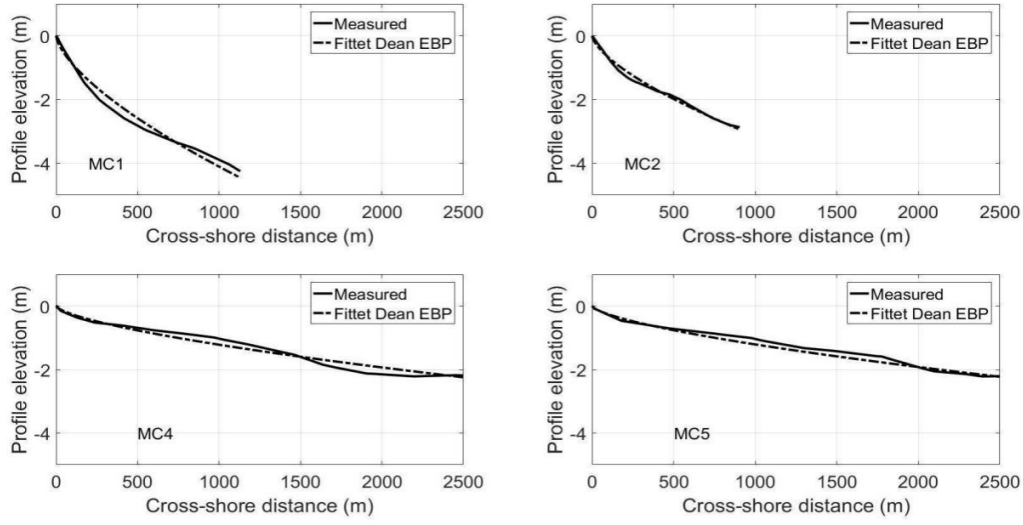

Figure 3. Comparison between measured cross-shore profiles (MC1, MC2, MC4, and MC5) and fitted EBP based on the formulation proposed by Dean [22].

Table 1. Results of least-squares fitting between measured beach profiles and the EBP formulation of Dean [22].

Profile	A ($m^{1/3}$)	D_{50} (mm)	E_{RMS} (m)
MC1	0.041	0.13	0.20
MC2	0.032	0.13	0.08
MC4	0.012	0.09	0.13
MC5	0.012	0.09	0.29

Note: A is the profile shape parameter related to sediment characteristics, D_{50} is the median sediment grain size (mm), and E_{RMS} is the root-mean-square deviation (m) between measured and fitted profiles.

2.3. Wave Climate

The deep-water wave climate in the Gulf of Tonkin exhibits distinct seasonal variability associated with the regional monsoonal wind regime. Based on visual buoy observations at Hon Dau station, waves predominantly approach from the north and northeast during the winter season, whereas wave directions are mainly from the east and southeast during summer under deep-water conditions [8, 10]. Correspondingly, mean deep-water wave heights range from about 1.8–2.0 m in winter and 1.2–1.4 m in summer [8, 10, 24]. Seasonal differences are most evident in the occurrence frequency of higher waves, with significant wave heights (Hs) exceeding 3 m about 10% of the time in winter, compared to Hs exceeding 2 m for a similar proportion during summer [8, 24]. Analysis of deep-water wave data from the GOWA reanalysis at the offshore station (**Figure 2**) further indicates that approximately 53% of the total wave energy propagates southward, corresponding to winter conditions, while about 47% propagates northward, representative of summer conditions.

Storms and typhoons affecting northern Vietnam predominantly occur during the summer months, particularly in July and August, with an average of about two events per year impacting the northern coastline. During such events, deep-water wave heights may reach 8–10 m, accompanied by storm surges of up to about 2 m [10, 21, 25].

Long-term in situ wave measurements remain limited in Vietnam, including the present study area. Available field observations were obtained through an international cooperation program between the Vietnam Institute of Hydrometeorology and the Russian Federation. Offshore buoy measurements were conducted along the central coast of Vietnam during 1999–2000 over a period of about three months. Data recorded at a buoy station located at a water depth of approximately 25 m (station VN06; see **Figure 1b**) during the winter period from October 1999 to January 2000 indicate that Hs exceeded 1.0 m for about 49% of the observation time and exceeded 1.5 m for approximately 23%.

The Gulf of Tonkin is connected to the South China Sea through a wide southeastern opening (**Figure 1b**), allowing swell waves generated under high-energy wave conditions in the South China Sea to propagate into the Gulf. Wave and wind measurements at anchored stations near the Day River estuary indicate that swell wave heights exceeding 1.0 m may occur even under low local wind speeds [24, 25], thereby indirectly influencing the Day River estuary coastline through incoming swell waves.

2.4. Tides

Field measurements indicate that astronomical tides in the study area are predominantly regular diurnal. Tidal waves propagate into the region from the South China Sea and are partially reflected within the northern enclosed part of the Gulf of Tonkin. Given a basin length of roughly 500 km and an average depth of about 50 m, the estimated resonance period is approximately 25 h [8, 26], which closely matches the diurnal tidal period. As a result, the diurnal constituents O1 and K1 are close to resonance, causing their amplitudes to increase northward along the Vietnamese coastline. The tidal range in the study area varies from around 0.5 m during neap tides to about 3.2 m during spring tides [26].

2.5. Current Regime

Nearshore currents are controlled by several main processes, including wave-induced currents, tidal currents, wind-driven circulation, and river outflow near river mouths. These processes interact with coastal morphology and produce complex current patterns in the

nearshore zone. Among them, tidal currents play the most important role in shaping tidal flats and tidal channels in low-lying coastal wetlands [8, 10].

In the Gulf of Tonkin, tidal waves mainly propagate from south to north, generating northward flood currents and southward ebb currents. In nearshore areas with water depths of about 5 m, average tidal current velocities range from 25 to 40 cm/s, while maximum velocities can reach 60–80 cm/s [10]. Because of tidal current asymmetry, the flood tide lasts for a shorter period than the ebb tide, accounting for approximately 42% and 58% of the tidal cycle, respectively. This asymmetry results in a net southward residual current along the coast [8].

Analyses based on field observations and numerical modelling show that wind-driven circulation in the Gulf of Tonkin forms a counterclockwise circulation pattern, centered in the middle of the gulf during both the summer and winter monsoon seasons [8]. This circulation results in persistent southward residual currents in the nearshore zone of the study area. Seasonal variations in wind velocity further influence this circulation, with higher wind velocities and stronger associated currents occurring in winter than in summer [8].

Long-term current monitoring along the Vietnamese coast remains limited, as most field surveys are conducted over relatively short periods, typically lasting from 2 to 7 days. In this study, current measurements were carried out at two anchored stations: an offshore station located seaward of the Day estuary at a water depth of 20 m, and a nearshore station situated south of the estuary at a depth of approximately 3 m (**Figure 2**). The measurements were conducted over a seven-day period, from 28 July to 4 August 2023. Analyses of current prisms based on the integrated dataset show a clear southward residual current at both stations. At the offshore station, current directions are generally aligned parallel to the coastline, whereas at the nearshore station, they are strongly influenced by local bathymetry and river discharge. Currents with velocities ranging from 30 to 50 cm/s occur with a frequency of 13.2% at the nearshore station and 4.2% at the offshore station. During the observation period, the mean current velocity at both stations was approximately 30 cm/s, while maximum velocities reached about 50–60 cm/s.

2.6. Riverine Sediment Budgets

The Red River supplies a large amount of sediment to the Gulf of Tonkin through seven active river mouths. Sediment discharge to the sea shows pronounced seasonal variability. Summer rainfall accounts for about 80% of the annual total, causing most sediment transport to occur during this season. Consequently, approximately 91–96% of the annual sediment load is delivered to the coastal zone in summer [8].

The total annual sediment input from the Red River to the sea is estimated to range from 75 to 100 Mt/yr. The relative contributions of sediment discharge from the main distributaries, arranged from north to south (**Figure 1a**), are about 19% from Van Uc, 6% from Thai Binh, 9% from Tra Ly, 21% from Ba Lat, 6% from Lach Giang, 19% from the Day River, and approximately 20% from the remaining smaller distributaries combined [8, 10, 27].

3. Shoreline Change Modelling

3.1. Shoreline Data

In this study, multi-temporal shoreline data covering the period from 1965 to 2023 were used to examine shoreline changes and alluvial plain development in the coastal area of the Day estuary. These data were derived from a combination of historical maps and satellite images. The study area includes Nghia Hung District in Nam Dinh Province and Kim Son District in Ninh Binh Province (**Figure 1a**). Shoreline positions were extracted for multiple years; however, only the most reliable datasets were selected for comparison with the model results. These datasets correspond to shoreline positions from the years 1965, 1989, and 2019.

3.2. Offshore Wave Data

Accurate characterization of offshore wave conditions is one of the main challenges in coastal process modelling. In Vietnam, long-term offshore wave measurements are generally not available. Therefore, this study used a 30-year offshore wave dataset (1993–2023) from GOWA [28] as input for the two-dimensional

wave transformation model [29]. The dataset has a time resolution of 1 h. GOWA, provided by the Copernicus Marine Service, supplies global wave data with a spatial resolution of 1/5° [28, 30]. This wave reanalysis covers the period from 1993 to 2023 and includes hourly wave parameters describing sea surface conditions. The wave data are produced using version 4 of the Mesoscale and Fine-scale WAve (MFWAM) model, which is driven by wind and atmospheric data from ECMWF ReAnalysis 5th generation (ERA5) [30, 31].

The offshore wave data were evaluated using wave measurements from the buoy station VN06 (**Figure 1b**). Because the measured wave direction at this station is considered unreliable, only wave height was used for the evaluation. A comparison of significant wave height between the VN06 observations and the GOWA data is shown in **Figure 4**. The results show good agreement, with a correlation coefficient of 0.8 and a mean absolute error of 0.23 m.

In this study, uncertainties related to deep-water wave data were not specifically analyzed. However, the comparison results indicate that the GOWA wave dataset is suitable for use in the study area. Previous studies have also shown that long-term GOWA wave data are reliable for wave climate studies and coastal engineering applications [31].

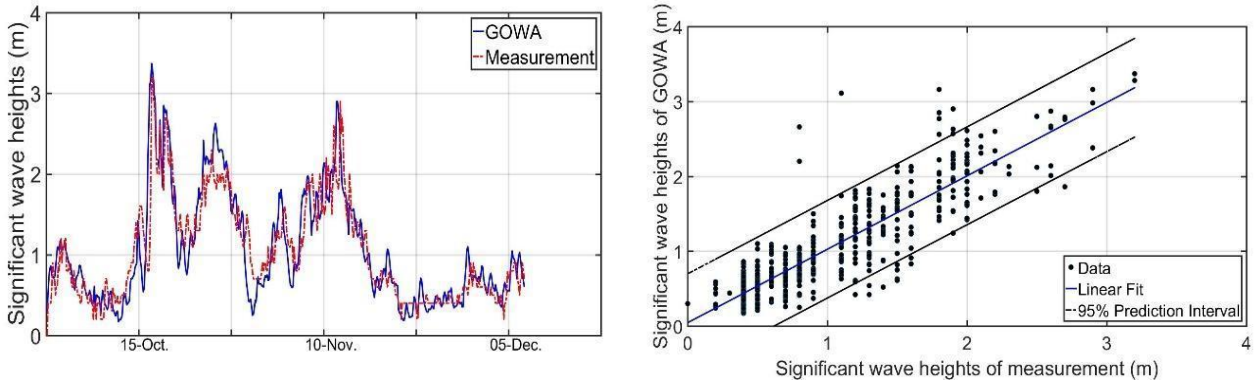

(a) **(b)**

Figure 4. Comparison between significant wave heights from GOWA and in situ measurements at the deepwater station VN06 during October–December 1999: (**a**) Time series comparison; (**b**) Linear regression with the 95% prediction interval.

3.3. Nearshore Wave Transformation

In this study, the nearshore wave climate was simulated using a two-dimensional Energy Balance Equation with a Diffraction term (EBED) model. The EBED model, developed by Mase [29], is derived from the energy balance equation for multidirectional random waves and incorporates the main physical processes governing wave transformation, including shoaling, refraction, diffraction, and wave breaking. A key advantage of the EBED model is its ability to reproduce wave transformation over complex bathymetry, together with its flexibility in handling a wide range of wave spectral inputs and outputs. To generate nearshore wave conditions for the study area, a 30-year hindcast time series of offshore wave data from GOWA was used as input to the EBED model.

The coastal geometry of the study area exhibits notable spatial variation. In the northern part of the Day estuary, the coastline is oriented in a northeast–southwest (NE–SW) direction, whereas south of the estuary, the coastline predominantly follows an east–west (E–W) orientation (**Figure 2**). Owing to this configuration, offshore waves approaching from the north (N) and northeast (NE) propagate in deep water, and part of their energy is transferred into the nearshore zone along the southern coast of the Day estuary through the combined effects of wave refraction and diffraction around the estuary headland. Wave observations from this study further indicate that onshore-directed waves are present in the nearshore area even when offshore waves and winds recorded at the BLV station mainly originate from the N or NE directions. Previous studies have shown that waves approaching from these two directions con-

tribute a substantial proportion, approximately 31%, of the total offshore wave energy [16]. Therefore, wave components from the N and NE directions must be considered in the nearshore wave transformation analysis. In general, two-dimensional wave transformation models can simulate wave propagation within an incident angle range of −90° to +90° relative to the offshore axis of the employed orthogonal coordinate system [29]. However, when the coordinate system is defined with the x-axis aligned parallel to the coastline in the east–west direction, waves approaching from the north and northeast cannot be adequately represented. To ensure that wave propagation from all relevant directions is properly simulated, two coordinate systems were implemented in the wave modelling framework. In the E–W coordinate system, the x-axis is oriented in the east–west direction, whereas in the NE–SW coordinate system, the x-axis is oriented along the northeast–southwest direction.

An evaluation was performed to quantify differences in wave propagation results obtained using the two coordinate systems. A representative wave case within the overlapping modelling region was selected, with a significant wave height of 1.55 m, a wave period of 5.3 s, and an incident wave direction of 145° relative to the north. In the E–W and NE–SW coordinate systems, the corresponding wave directions are 55° and 100°, respectively. This wave condition was simulated independently using both coordinate systems. For comparison, the results from the NE–SW coordinate system were transformed into the N–W coordinate system, which is used in the shoreline evolution model. Differences in significant wave height and wave propagation direction along the 6 m depth contour (representing the depth of closure) are shown in **Figure 5**, respectively. Differences in wave period were negligible and are therefore not discussed further. The comparison shows that the maximum difference in significant wave height is 0.07 m, and the maximum difference in wave direction is 3.1°. These small discrepancies indicate that the influence of using different coordinate systems on the wave propagation results is minor. Similar conclusions have been reported in previous studies [16].

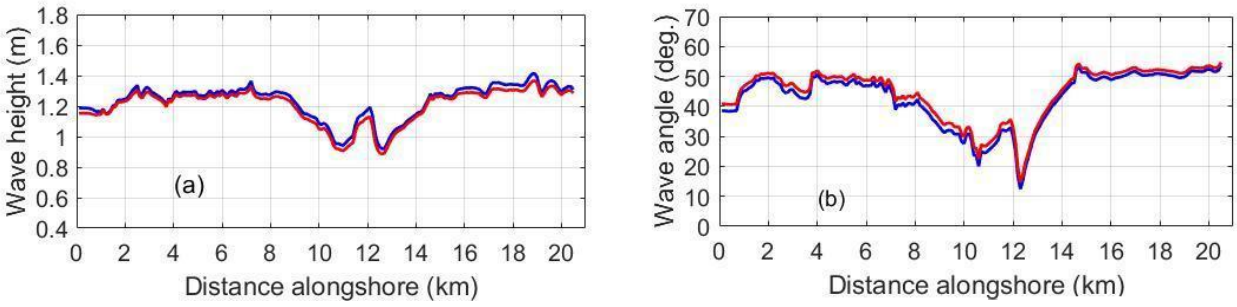

(a) **(b)**

Figure 5. Comparison of simulated wave transformation results along the 6-m depth contour using two coordinate systems. The E–W and NE–SW coordinate systems are represented by the blue and red lines, respectively: (**a**) Wave height and (**b**) Wave direction.

3.4. Sediment Transport and Shoreline Change Model

Several previous studies have applied different approaches to estimate longshore sediment transport and shoreline change along the coast from the northern part of the Day estuary to the Ba Lat estuary (**Figure 1**). Häglund and Svensson [32] employed the CERC formula [33] to calculate longshore gradients in sediment transport. In their approach, a one-dimensional wave transformation model was used to reproduce longshore wave conditions for different shoreline orientations and to estimate sediment transport rates. However, this method does not explicitly account for spatial variations in breaking wave height along the shoreline.

The BIJKER formula [34] was applied by Pruszak et al. [10] and Wijdeven [35] to compute discrete sediment transport rates at selected locations along the coast. In addition, the shoreline change model GENESIS (Generalized Model for Simulating Shoreline Evolution) was used

by Donnelly et al.[36] to simulate sediment transport rates and shoreline evolution along the coastal stretch between the Lach Giang and Ha Lan estuaries (**Figure 1a**). In the GENESIS model, sediment transport rates for individual shoreline cells are calculated using a modified version of the CERC formula that incorporates the longshore gradient of breaking wave height.

In the present study, a numerical model based on the one-line theory of shoreline change, as developed by Hoan et al.[16], is applied. The numerical algorithms used in this model were originally formulated by Hanson and Kraus[37]. The governing equation of the model is expressed as follows:

$$\frac{\partial y}{\partial t} + \frac{1}{(D_B + D_c)}\left[\frac{\partial Q}{\partial x} + q\right] = 0 \qquad (1)$$

where: x = longshore coordinate (m); y = cross-shore shoreline position (m); t = time (s); D_B = average berm elevation (m); D_c = Depth of closure (m); Q = LST rate (m^3/s); q = source or sink of sand ($m^3/s/m$).

The empirical predictive formula for the longshore sand transport is expressed as

$$Q = \left(H^2 C_g\right)_b \left[a_1 Sin2\theta_{bs} - a_2 Cos\theta_{bs}\frac{\partial H}{\partial x}\right]_b \qquad (2)$$

where: H = wave height (m); C_g = wave group celerity given by linear wave theory (m/s); b = subscript denoting breaking wave condition; θ_{bs}= angle of breaking waves to the local shoreline; and:

$$a_1 = \frac{K_1}{16(\rho_s/\rho - 1)(1-p)(1.416)^{5/2}} \qquad (3)$$

$$a_2 = \frac{K_2}{8(\rho_s/\rho - 1)(1-p)tan\,\beta\,(1.416)^{5/2}} \qquad (4)$$

where: K_1, K_2 = empirical coefficients, treated as calibration parameters; ρ_s = density of sand (kg/m^3); ρ = density of water (kg/m^3); p = porosity of sand on the bed; $tan\ \beta$ = average bottom slope from the shoreline to the depth of active longshore transport.

Field observations from the adjacent Hai Hau coast reported by Donnelly et al.[36] indicate that part of the fine-grained sediment is lost offshore under erosional conditions. By comparing sediment grain-size characteristics, measured beach profiles, and theoretical equilibrium profiles, Donnelly et al.[36] showed that the measured profiles were consistently lower than those predicted from grain-size considerations. This discrepancy was interpreted as evidence of offshore loss of fine sediment and suggested that including an erosion-dependent offshore loss term could improve simulations of long-term shoreline evolution in accretion–erosion transition zones. This formulation was subsequently applied by Hoan et al.[16] for the Hai Hau coastal area, demonstrating its suitability for simulating long-term shoreline evolution in this region.

Based on this concept, offshore sediment loss is assumed to depend on gradients in LST through an offshore loss parameter α, which specifies the ratio of fine material in the eroded sediment. A positive LST gradient ($\partial Q/\partial x > 0$) indicates sediment divergence and shoreline erosion, during which a fraction of the mobilized fine sediment is transported beyond the active beach profile and lost to deeper waters. In contrast, a negative LST gradient ($\partial Q/\partial x < 0$) represents sediment convergence and accretion, under which offshore sediment loss is neglected. Accordingly, offshore sediment loss is parameterized as follows[36].

$$q = \frac{\alpha}{1-\alpha}\frac{\partial Q}{\partial x},\ \frac{\partial Q}{\partial x} > 0 \qquad (5)$$

$$q = 0,\qquad \frac{\partial Q}{\partial x} < 0 \qquad (6)$$

By substituting these expressions into Equation (1), the sediment continuity equation can be rewritten as:

$$\frac{\partial y}{\partial t} + \frac{1}{(D_B + D_c)}\frac{1}{(1-\alpha)}\frac{\partial Q}{\partial x} = 0 \qquad (7)$$

3.5. Modelling Setup

Due to the availability of shoreline data, the model application area was defined from the southern side of the Lach Giang estuary to the southern side of the Lach Truong estuary (**Figure 1a**). This coastal segment includes a variety of coastal features and processes, including: (a) sediment transport and morphological development at both regional and local scales; (b) spatially and temporally varying cross-sectional areas of tidal flats,

with periodic opening and closing of tidal channels; (c) significant shoreline response within tidal flat areas; and (d) substantial sediment input from river mouths as well as from the north through longshore sediment transport [14, 15, 18, 20].

The numerical model was applied to perform two main types of simulations: (1) simulation of the annual net longshore sediment transport and (2) simulation of shoreline evolution at the regional scale and in the vicinity of river mouths. The objective of these simulations was to examine the response of the shoreline to sediment supply from the river system under the influence of coastal hydrodynamic conditions. In addition, the simulations were used to determine the longshore sediment transport coefficient, which provides a basis for assessing the coastal sediment budget.

The total shoreline length of the study area is approximately 25 km. A model coordinate system was defined with the x-axis oriented in the east–west direction and the y-axis oriented southward. Lateral boundary conditions were specified such that the southern boundary, located near the Lach Truong estuary, was treated as a fixed boundary with no shoreline change. In contrast, the northern boundary was defined as a movable boundary because no stable reference point could be identified at this end of the domain. Therefore, shoreline variations at the northern boundary were prescribed based on observed shoreline positions from 1965 to 2019, following the moving-boundary approach proposed by Hanson and Kraus [37]. The spatial resolution of the model was set to 100 m.

A hindcast wave dataset covering approximately 30 years (1993–2023) with a temporal resolution of 1 h, provided by GOWA, was used as input for the 2D EBED model. Longshore wave breaking parameters, including water depth, wave height, wave direction, wave period, and group velocity, were derived from the EBED model and used as input for the shoreline change model. The depth of closure was determined using empirical formulations based on the wave height exceeded for 12 h/y [37–39]. Statistical analysis of offshore wave height data indicated a depth of closure of approximately 6.0 m. The mean sediment grain size along the shoreline ranges from 0.09 to 0.13 mm [23].

Sediment sources within the study area include fluvial sediment input from river mouths and longshore sediment transport from the north. Based on previous studies [8, 10, 20, 27], the sediment source boundary conditions were specified as $10{,}000 \times 10^3$ m^3/y for the Day estuary, $1{,}000 \times 10^3$ m^3/y for the Can estuary, and 500×10^3 m^3/y for the Truong estuary. According to the modelling results reported by Hoan et al. [16], the longshore sediment transport from Hai Hau Beach to the northern side of the Day estuary is approximately 200×10^3 m^3/y.

Several studies have demonstrated that the construction of the Hoa Binh Dam on the Red River has significantly reduced sediment supply to downstream areas. Analyses of measured suspended sediment data indicate that the total suspended sediment load of the Red River system decreased by about 20–40% after the completion of the Hoa Binh Dam in 1983 [11, 12, 27]. This reduction was incorporated into the model by decreasing the sediment input from the Day estuary by 30% for the period after 1983.

4. Model Results

An implicit numerical scheme was applied in the shoreline change model with a spatial resolution of 100 m and a computational time step of 0.5 h, following the approach described by Hoan et al. [16]. Model calibration and validation were conducted using measured shoreline positions from 1965, 1989, and 2019 along the Day estuary beach. Model stability was assessed using the stability parameter (Rs) based on the Courant criterion [37], for which values below 10 are generally considered acceptable. In the simulations, Rs was computed at all shoreline grid points at each time step, and the maximum value was evaluated. The maximum Rs value reached 5.2 for both simulation phases, confirming stable numerical performance.

The model time step was selected to ensure consistency with the temporal resolution of the input wave data. In this study, the wave hindcast data have a time interval of 1 h, while the model time step is 0.5 h. Thus, new wave input data were applied to the model after every two computational steps.

The agreement between modelled and measured

shorelines was evaluated using two error metrics: the maximum absolute error (m) and the average relative error (%). The maximum absolute error represents the largest absolute distance between the modelled and measured shoreline positions. The average relative error was calculated using the following expression:

$$Error\ (\%) = \frac{\frac{1}{n}\sum_{i=1}^{n}\left|y_{modelled}^{(i)} - y_{measured}^{(i)}\right|}{\frac{1}{n}\sum_{i=1}^{n}\left|y_{eroded}^{(i)}\right|} \times 100 \quad (8)$$

where n = number of cells alongshore; $y_{modelled}^{(i)}$ = modeled shoreline position of cell, i; $y_{measured}^{(i)}$ = measured shoreline position of cell, i; $y_{eroded}^{(i)}$ = distance between the measured initial and final shorelines, respectively, in cell i.

4.1. Model Calibration and Validation

The measured shoreline positions from 1965 and 1989 were used to calibrate the model. During the calibration period, three parameters were evaluated, including the offshore sediment loss coefficient α and two empirical coefficients, K_1 and K_2, in the longshore sediment transport formulation. The coefficient α was set to 0.7 following the approach proposed by Donnelly et al.[36] and based on sediment characteristics and equilibrium beach profiles reported for the study area[20, 23].

The coefficient K_2 was selected as a fraction of K_1, within the commonly applied range of 0.4–0.6 K_1 suggested by Hanson and Kraus[37]. In the study area, K_2 shows relatively low sensitivity. Therefore, the calibration mainly focused on the coefficient K_1, which was determined by minimizing the mean squared error between the modelled and measured shorelines (**Figure 6**).

The final calibrated parameter values are α = 0.7, K_1 = 0.85, and K_2 = 0.40. For the calibration period, the maximum absolute error and the average relative error were 650 m and 9.2%, respectively (**Table 2**). Based on shoreline measurements between 1965 and 1989, the maximum accretion rate was 125 m/y, while the average accretion rate was 73 m/y (**Table 2**).

Using the calibrated parameter set, the model was validated for the period from 1989 to 2019, with the measured shoreline position in 1989 used as the initial condition (**Figure 7**). For the validation period, the maximum absolute error and the average relative error were 755 m and 12.5%, respectively (**Table 2**). Based on shoreline measurements between 1989 and 2019, the maximum accretion rate was 225 m/y, while the average accretion rate was 111 m/y (**Table 2**). The modelled spatial distribution of annual mean LST along the study coastline is shown in **Figure 8**.

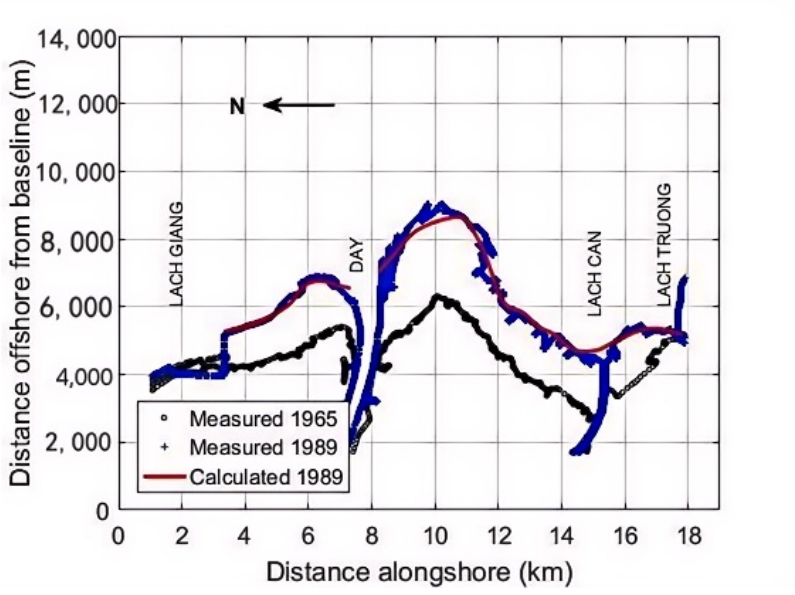

Figure 6. Comparison between modelled and measured shorelines for the period 1965–1989.
Note: The black line indicates the measured shoreline in 1965, used as the initial condition for the model; the blue line shows the measured shoreline in 1989, and the red line shows the modelled shoreline for 1989.

Table 2. Summary of shoreline errors and accretion rates for the calibration and validation periods.

	Max Absolute Error (m)	Average Relative Error (%)	Max Accretion Rate (m/y)	Average Accretion Rate (m/y)
Calibration	650	9.2	125	73
Validation	755	12.5	225	111

Note: Accretion rates were calculated from changes in measured shoreline positions along the model grid for the calibration period (1965–1989) and the validation period (1989–2019).

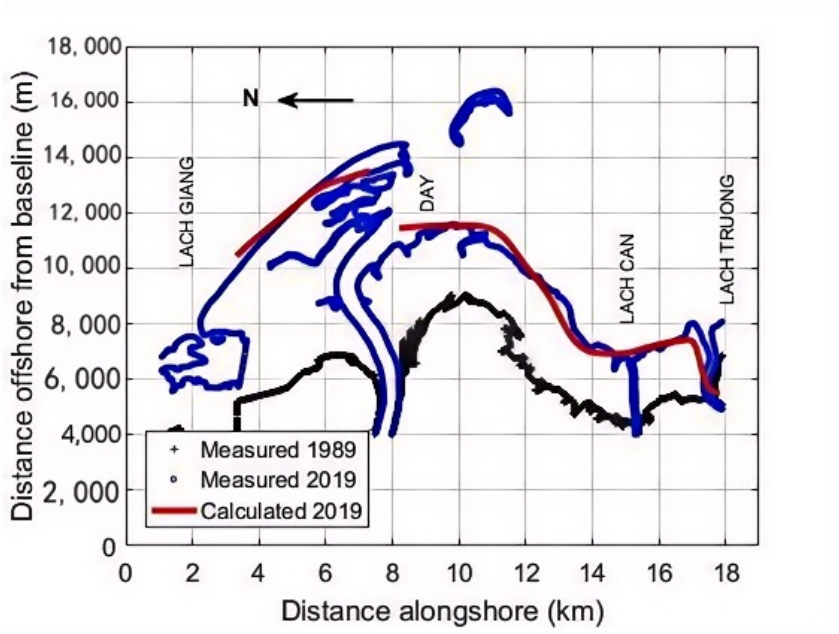

Figure 7. Comparison between modelled and measured shorelines for the period 1989–2019.
Note: The black line indicates the measured shoreline in 1989, used as the initial condition for the model; the blue line shows the measured shoreline in 2019, and the red line shows the modelled shoreline for 2019.

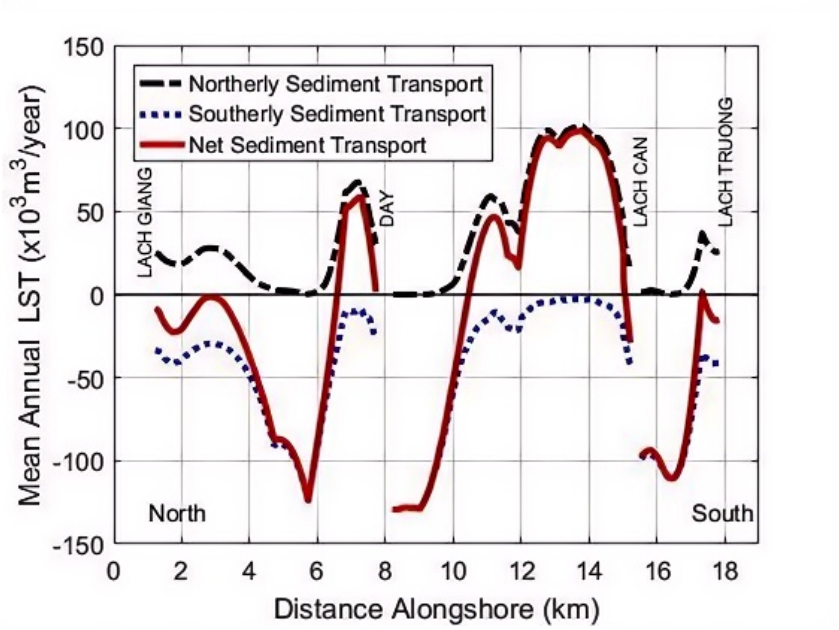

Figure 8. Spatial distribution of modelled annual LST rates ($\times 10^3$ m^3/y) along the study coastline, with positive values indicating transport toward the north.

4.2. Modelled Sediment Budget

The sediment budget analysis quantifies the main sediment inputs and outputs within the study area (**Figure 9**). The total sediment input is calculated as the sum of sediment supplied by the river system (Q_{river}), LST entering the domain from the south ($Q_{south(in)}$) and from the north ($Q_{north(in)}$), resulting in a total input of $Q_{source} = 11{,}566 \times 10^3$ m^3/y.

The total sediment output consists of LST leaving the domain toward the north ($Q_{north(out)}$) and toward the south ($Q_{south(out)}$), as well as sediment loss to the offshore waters of the study area (Q_{off}). The total sediment output is therefore $Q_{sink} = 2{,}059 \times 10^3$ m^3/y.

Based on these values, the net annual sediment volume deposited along the beach is estimated as the difference between total input and output, yielding $Q_{source} - Q_{sink} = 9{,}507 \times 10^3$ m^3/y. This corresponds to approximately 82% of the total sediment input, indicating that most of the supplied sediment is retained within the coastal system. Wave-induced longshore sediment transport accounts for about 1% of the total sediment exchange, while offshore sediment loss represents approximately 17% of the total river-supplied sediment.

Offshore sediment loss (Qoff) was estimated using an erosion-rate-dependent formulation proposed by Donnelly et al.[36], as described by Equations (5) and (6). Offshore sediment loss was evaluated at each alongshore grid cell and at each computational time step. When erosion conditions occurred, Equation (5) was applied to estimate the sediment volume transported into the deeper offshore waters. The total offshore sediment loss was then obtained by integrating these contributions over space and time.

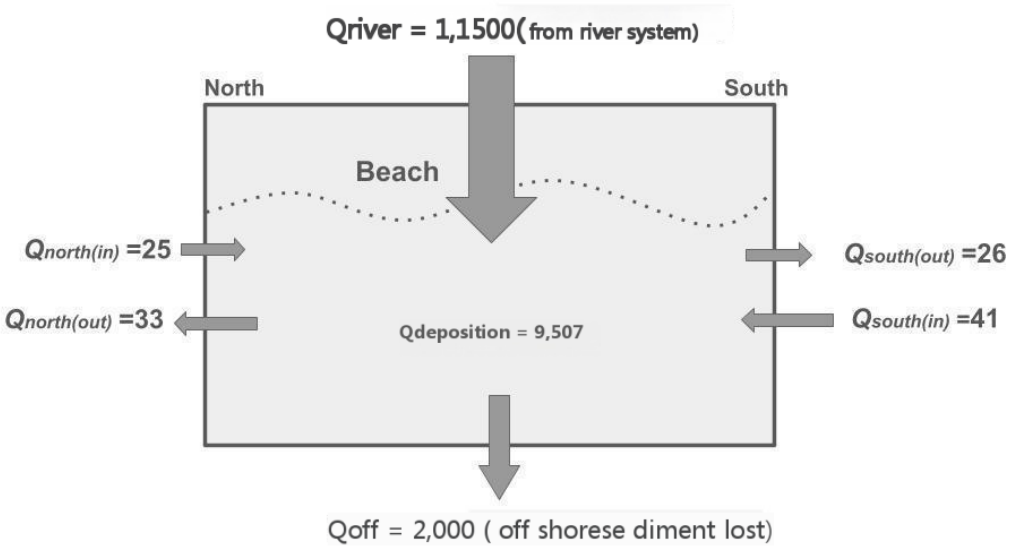

Figure 9. Schematic diagram of the calculated sediment budget for the study area, showing sediment input from the river system, alongshore sediment exchange from the north and south, deposition within the beach area, and sediment loss to the offshore.

Note: Values are multiplied by 10^3 m^3/y.

4.3. Net Sediment Transport Pathways

Based on the simulated net sediment transport results (**Figure 8**), a schematic map illustrating the general sediment transport trends is presented in **Figure 10**. In **Figure 8**, the net sediment transport (bold red line) follows the sign convention adopted in the model, where negative values indicate southward transport and positive values indicate northward transport.

From Lach Giang to the Day estuary, the net sediment transport changes from negative to positive (**Figure 8**), corresponding to southward transport from Lach Giang and northward transport from the Day estuary (**Figure 10**). Between the Day and Lach Can estuaries, the transport again shifts from negative to positive, indicating southward transport from the Day estuary and northward transport from Lach Can. In contrast, between Lach Can and Lach Truong, the net sediment

transport remains negative, indicating persistent southward transport.

Overall, the modelled sediment transport pattern indicates that sediment supplied by the Day River is redistributed alongshore toward both the northern and southern coastal segments.

The modelled transport patterns also indicate the presence of sediment convergence zones around the Day estuary, where river-derived sediment interacts with LST from adjacent coastal segments. These convergence zones correspond to areas of sediment accumulation and the development of spits and other depositional features near the estuary.

For comparison, the net sediment transport directions reported by Duc et al.[15] are reproduced in **Figure 10**. However, in the area from Lach Can toward Lach Truong, these directions could not be reproduced because the corresponding data were not reported.

Figure 10. Net sediment transport pathways.

Note: Arrow directions indicate the transport direction only and do not represent transport magnitude. Yellow arrows indicate pathways derived from the present model, while white arrows indicate pathways reproduced from Duc et al.[15]. No data are available from Duc et al.[15] for the coastal segment between Lach Can and Lach Truong.

5. Discussion

5.1. Morphodynamic Setting of the Red River Delta

The Red River Delta is a low-lying coastal plain located between several sediment-rich river mouths and directly connected to the South China Sea[12, 14]. The area is influenced simultaneously by river discharge, waves, and tides. The interaction between hydrodynamic and morphodynamic processes has created a highly dynamic coastal system. As a result, zones of accretion and erosion alternate in both space and time[12, 14].

In sediment-rich delta systems, river mouths can act as important sediment sources that support shoreline stability and enhance resistance to wave-induced erosion when sediment supply is continuously maintained[12]. Strong accretion commonly occurs at river mouths such as the Day and Ba Lat estuaries, while severe erosion has been recorded in several coastal sections, particularly at Hai Hau[10, 14]. The large riverine sediment supply promotes rapid tidal-flat development and coastal accretion in the Red River Delta[8]. These newly accreted areas are often used for agriculture and aquaculture. However, large sediment loads delivered by the rivers can also promote rapid sediment deposition near river mouths, potentially leading to channel shoaling and navigation constraints[9, 27, 40].

Under these conditions, the demand for channel regulation and coastal protection measures has increased. In the Red River Delta, the existing protection

system mainly relies on sea dikes and breakwaters. However, the performance of these structures is not always stable, and periodic damage has been reported, particularly along the Nam Dinh coastline [41, 42]. This situation poses significant challenges for long-term channel management and coastal protection. It also suggests that local engineering solutions alone may not be effective unless they are considered within the framework of regional sediment continuity, as estuarine coastal systems are strongly interconnected through both longshore and cross-shore sediment transport processes.

5.2. Model Performance and Sediment Transport

In the present study, long-term wave hindcast data of the GOWA provided by Copernicus Marine Environment Monitoring Service (CMEMS) were used to downscale nearshore waves in the study area using the EBED model. This approach provided detailed wave conditions and reliable estimates of LST rates in the region, resulting in good agreement between simulated shoreline evolution and measured data.

The simulated net sediment transport (**Figure 8**) shows that riverine sediment is transported away from the river mouth in both directions along the coast, forming convergence zones between adjacent estuaries (**Figure 10**). This transport pattern is consistent with the independent analysis of Duc et al. [15]. While Duc et al. [15] identified long-term transport trends based on sediment characteristics, the present study quantifies both the direction and magnitude of net sediment transport by considering the combined influence of wave forcing and riverine sediment supply. This agreement strengthens the reliability of the simulation results. Although a simplified one-line approach is applied, the model reasonably reproduces the magnitude and overall trend of long-term shoreline change.

5.3. Sediment Budget

The sediment budget analysis shows that riverine sediment supply dominates the system, while the annual mean longshore sediment transport contributes around 1% of the total sediment exchange. This suggests that the study area is a strongly accretionary system mainly controlled by sediment inputs from the rivers [12, 14].

The small contribution of longshore sediment transport indicates that cross-shore transport and sediment exchange between offshore bars and the shoreline may play a more important role in maintaining morphodynamic balance. Sediment delivered by rivers and transported offshore may return to the nearshore zone through ebb shoal and bar attachment processes, thereby contributing to the dynamic equilibrium of the estuary [43]. This highlights the need to fully consider three-dimensional sediment pathways in estuarine sediment management.

5.4. Seasonal Variability and Extreme Events

The results presented above are based on annual averages and therefore do not fully capture seasonal variability. The study area exhibits a pronounced seasonal pattern, with most of the annual suspended sediment load transported during the rainy season from May to October [8, 27]. During this period, high river discharge and elevated sediment concentrations dominate the accretion trend and promote the development of offshore sandbars near the river mouth. In contrast, during the dry season, river discharge decreases significantly, while the northeast monsoon increases oblique wave incidence and enhances southward LST [10, 12]. Under these dry-season conditions, LST becomes relatively more important than riverine sediment supply, leading to sediment redistribution and the formation of spits and river-mouth bars at the estuary, and contributing to seasonal channel shoaling and infilling. Overall, the morphodynamic behavior of the Day estuary reflects the interaction between two dominant seasonal regimes. During the rainy season, shoreline evolution is mainly controlled by riverine sediment supply. During the dry season, waves and LST exert a stronger influence by redistributing river-derived sediment along the coast. Consequently, effective estuarine management and the design of coastal protection structures should consider the regional sediment balance and sediment-cell connectivity to ensure long-term morphological sustainability.

As mentioned in Section 3.5, sediment discharge

from the Red River decreased by approximately 30% after 1983 following the completion of the Hoa Binh Dam [27]. Despite this reduction, beach accretion during the period 1989–2019 was more pronounced than during 1965–1989, particularly along the coast from the Day estuary to Lach Giang (**Figures 6** and **7**). This enhanced accretion is unlikely to be explained solely by reduced fluvial sediment input. It may also be associated with extreme events that promoted additional sediment redistribution and coastal deposition, as well as broader morphodynamic adjustments of the delta system.

On average, approximately 12 typhoons affect the South China Sea each year [21]. They occur mainly during the summer months and often reach high intensity in the northern South China Sea, including the present study area. These events generate high-energy waves that reshape the shoreline and beach morphology, frequently causing substantial short-term erosion. Heavy rainfall and upstream landslides associated with these storms can also increase fluvial sediment discharge to the coastal zone, contributing to shoreline evolution. In addition, the seasonal monsoon system produces prolonged periods of strong waves and elevated LST, promoting the development of sand spits along the coast. Although this study does not analyze individual extreme events, extreme wave conditions associated with typhoons and monsoons are incorporated into the estimation of LST and shoreline evolution.

5.5. Implications for Sustainable Marine Structures

In the context of rapid sedimentation at river mouths, the demand to maintain navigation depth has increased. Hard coastal structures such as detached breakwaters, groynes, seawalls, and jetties are widely implemented to protect the shoreline and control sediment deposition, particularly at estuaries [42, 44, 45]. Jetties can concentrate river flow and shift the river-mouth bar offshore, potentially contributing to a more stable navigation channel. However, these structures can disrupt natural sediment transport pathways, leading to sediment deficits in downdrift areas and causing localized erosion [46, 47]. This reflects an inherent trade-off between maintaining navigability and preserving the regional sediment balance in engineered estuarine systems [42, 48]. By redirecting sediment offshore, such interventions may enhance sediment loss to deeper waters and reduce sediment recycling within the nearshore system. They may also limit tidal-flat development and affect long-term morphodynamic stability [12].

These limitations highlight the need to evaluate estuary regulation measures based on sediment balance and long-term morphodynamic impacts rather than focusing solely on channel depth. Engineering solutions should be considered within a system-scale morphodynamic framework, with priority given to maintaining sediment continuity and managing sediment at the sediment-cell scale [49], rather than pursuing local stabilization. The growing adoption of hybrid approaches that combine hard structures with nature-based elements reflects a more balanced approach to engineering effectiveness and ecological sustainability [50, 51]. The modeling framework developed in this study provides a quantitative basis for supporting the long-term design and assessment of such interventions.

5.6. Model Limitations

Several limitations of this study should be acknowledged. Tidal currents and river discharge were not explicitly simulated. Net sediment transport induced by tides over a full tidal cycle is typically small and is therefore often neglected in one-line shoreline models [37]. Nevertheless, tidal processes may still influence tidal-flat development under complex geomorphological conditions. River discharge may also enhance the offshore transport of fine sediment, potentially contributing to sediment loss to deeper waters.

In addition, the sensitivity and stability of the calibration coefficients were not systematically evaluated. The selected parameters (α = 0.7; K_1 = 0.85; K_2 = 0.40) are comparable to values reported for the adjacent Hai Hau coast, where offshore wave conditions are similar. This indicates that the adopted parameter set is physically reasonable. However, a detailed sensitivity analysis would be required in future studies to further assess model robustness.

6. Conclusions

The shoreline change model successfully reproduces shoreline evolution at the Day estuary beach from 1965 to 2019, capturing the main features of the complex coastal morphology associated with multiple river mouths. The simulated shoreline changes show good agreement with observations during both the calibration and validation periods.

The modelled sediment budget indicates that riverine sediment input is the dominant driver of coastal accretion in the study area, while wave-induced LST plays a secondary role. Waves and associated coastal processes mainly redistribute river-derived sediment alongshore and cross-shore, with a portion transported offshore into the deeper waters.

Although the model represents long-term average conditions, sediment dynamics in the study area are known to exhibit strong seasonal variability, with river discharge dominating sediment supply during the rainy season and wave-driven LST becoming more important during the dry season.

These findings provide new insights into sediment transport pathways and morphodynamic processes in the study area and offer a quantitative basis for coastal management and the design of sustainable marine structures in river-mouth environments. However, the results should be interpreted in the context of the simplified one-line modelling framework, which does not explicitly represent tidal currents and river flow dynamics.

Author Contributions

All authors contributed equally to the conception, design, data collection, analysis, and writing of this study. All authors have read and agreed to the published version of the manuscript.

Funding

This study was funded by the Ministry of Agriculture and Rural Development of Vietnam under the Science and Technology Project for the period 2023–2025, entitled "Research and assessment of coastal evolution in the Day estuary area and proposal of management measures".

Institutional Review Board Statement

Not applicable.

Informed Consent Statement

Not applicable.

Data Availability Statement

The data used in this study are available from the corresponding author upon reasonable request.

Acknowledgments

The authors gratefully acknowledge Professor Magnus Larson, Dr. Grégoire O. Abessolo, and M. Sc. Nguyen Thi Hai for their valuable discussions and constructive comments on the manuscript.

Conflicts of Interest

The authors declare no conflict of interest.

AI Use Statement

The authors used AI-assisted language-editing tools (ChatGPT by OpenAI and Microsoft Copilot, 2025 versions) solely for grammar checking, sentence structure refinement, and improving the readability of the English text in this manuscript. The authors take full responsibility for all academic content, including all ideas, data, analyses, and conclusions presented herein. The use of AI was thoroughly reviewed and supervised by the authors.

References

[1] Jokhu, J.R., Fernando, A., Hamzah, D.A., et al., 2025. Integrating community empowerment, ecotourism, and maritime resilience for a sustainable blue economy. Maritime Technology and Research. 7(4), 279–344. DOI: https://doi.org/10.33175/mtr.2025.279344

[2] Rozaki, Z., Man, N., Sofani, N., et al., 2025. The com-

munity's role in the coastal tourism economy of Yogyakarta, Indonesia. Maritime Technology and Research. 7(4), 276–615. DOI: https://doi.org/10.33175/mtr.2025.276615

[3] Turriza, R.A.C., Fernández-Díaz, V.Z., Rojas, D.M.C., et al., 2024. Coastal vulnerability assessment with a hierarchical coastal segments approach. Ocean & Coastal Management. 249, 106989. DOI: https://doi.org/10.1016/j.ocecoaman.2023.106989

[4] Cruz-Ramírez, C.J., Chávez, V., Silva, R., et al., 2024. Coastal management: A review of key elements for vulnerability assessment. Journal of Marine Science and Engineering. 12(3), 386. DOI: https://doi.org/10.3390/jmse12030386

[5] Mathew, V., Agarwala, N., 2025. Impact of climate change on coastal communities and security. Maritime Technology and Research. 7(4), 277–917. DOI: https://doi.org/10.33175/mtr.2025.277917

[6] Feng, X., Zhu, C., Liu, J.P., et al., 2023. Sediment Dynamics in Coastal and Marine Environments: Scientific Advances. Water. 15(7), 1404. DOI: https://doi.org/10.3390/w15071404

[7] Wright, L.D., Thom, B.G., 2023. Coastal Morphodynamics and Climate Change: A Review of Recent Advances. Journal of Marine Science and Engineering. 11(10), 1997. DOI: https://doi.org/10.3390/jmse11101997

[8] van Maren, D.S., Hoekstra, P., 2004. Seasonal variation of hydrodynamics and sediment dynamics in a shallow subtropical estuary: The Ba Lat River, Vietnam. Estuarine, Coastal and Shelf Science. 60(3), 529–540. DOI: https://doi.org/10.1016/j.ecss.2004.02.011

[9] Dong, M.D., Poizot, M., Cuong, D.H., et al., 2023. Transport trend of recent sediment within the nearshore seabed of Hai Hau, Nam Dinh province, southwest Red River Delta. Frontiers in Earth Science. 11, 1099730. DOI: https://doi.org/10.3389/feart.2023.1099730

[10] Pruszak, Z., Szmytkiewicz, M., Hung, N.M., et al., 2002. Coastal Processes in the Red River Delta Area, Vietnam. Coastal Engineering Journal. 44(2), 97–126. DOI: https://doi.org/10.1142/S0578563402000469

[11] Quang, N.H., Manh, T.X., Viet, T.Q., et al., 2026. Five decades of shoreline dynamics and their response to dramatically reduced sediment supply on the southern Red River Delta coast, Vietnam. Estuaries and Coasts. 49, 15. DOI: https://doi.org/10.1007/s12237-025-01640-y

[12] van Maren, D.S., 2005. Barrier formation on an actively prograding delta system: The Red River Delta, Vietnam. Marine Geology. 224(1–4), 123–143. DOI: https://doi.org/10.1016/j.margeo.2005.07.008

[13] Quang, N.H., Thang, N.H., An, N.V., et al., 2023. Delta lobe development in response to changing fluvial sediment supply by the second largest river in Vietnam. Catena. 231, 107314. DOI: https://doi.org/10.1016/j.catena.2023.107314

[14] Fan, D., Nguyen, D.V., Su, J., et al., 2019. Coastal morphological changes in the Red River Delta under increasing natural and anthropic stresses. Anthropocene Coasts. 2, 51–71. DOI: https://doi.org/10.1139/anc-2018-0022

[15] Duc, D.M., Nhuan, M.T., Ngoi, C.N., et al., 2007. Sediment distribution and transport at the nearshore zone of the Red River delta, Northern Vietnam. Journal of Asian Earth Sciences. 29(4), 558–565. DOI: https://doi.org/10.1016/j.jseaes.2006.03.007

[16] Hoan, L.X., Hanson, H., Larson, M., et al., 2010. Modelling Shoreline Evolution at Hai Hau Beach, Vietnam. Journal of Coastal Research. 26(1), 31–43. DOI: https://doi.org/10.2112/08-1061.1

[17] Cham, D.D., Son, N.T., Minh, N.Q., 2013. Application of remote sensing technology and geographic information system in assessing the changes of coastal alluvial plains of Cua Day over period (1966–2011). Journal of Earth Sciences. 35(4), 349–356. Available from: https://vjs.ac.vn/jse/article/view/4119

[18] Son, Q.P., Anh, N.D., 2016. Erosion-accretion evolution of Hai Hau coastal area (Nam Dinh province) and neighboring areas over the past 100 years based on analysis of topographic maps and multitemporal remote sensing data. Vietnam Academy of Science and Technology: Journal of Earth Sciences. 38(1), 118–130. Available from: https://vjs.ac.vn/jse/article/view/7852/pdf (in Vietnamese)

[19] Hung, D.B., Dang, V.H., Pha, P.D., et al., 2020. Studying and forecasting the evolution of the Day River coastal zone up to the year 2070. Journal of Marine Science and Technology. 20(1), 39–49. DOI: https://doi.org/10.15625/1859-3097/20/1/12668

[20] Huu, V.C., Ha, D.T., Hoan, L.X., 2023. Estimation of sediment transport along the coast of the coastal area of Nghia Hung (Nam Dinh) and Kim Son (Ninh Binh). Vietnam Journal of Science and Technology. 90(Special Issue 2023), 90–98. Available from: https://vjol.info.vn/index.php/vawr/article/view/105190 (in Vietnamese)

[21] Le, M.D., Vlasova, G., Nguyen, D.T.T., 2021. Distribution features of the typhoons in the South China Sea. Russian Journal of Earth Sciences. 21(1), ES1001. DOI: https://doi.org/10.2205/2020es000746

[22] Dean, R.G., 1991. Equilibrium Beach Profiles: Characteristics and Applications. Journal of Coastal Research. 7(1), 53–84. Available from: http://www.

jstor.org/stable/4297805

[23] Thanh, D.X., Quan, N.H., Trang, N.T.H., et al., 2024. Grain-size Characteristics and Net Transport Patterns of Surficial Sediments in the Day River Estuary. VNU Journal of Science: Earth and Environmental Sciences. 40(2), 105–115. DOI: https://doi.org/10.25073/2588-1094/vnuees.5103 (in Vietnamese)

[24] Sjödahl, M., Kalantari, Z., 2005. Nearshore Hydrodynamics at Hai Hau Beach, Vietnam: Field Measurements and Wave Modelling [Master's Thesis]. Lund University: Lund, Sweden. p. 83. Available from: https://www.lunduniversity.lu.se/lup/publication/1326248

[25] Sundstrom, A., Sodervall, E., 2004. The Impact of Typhoon on the Vietnam Coastline—A Case Study of Hai Hau and Ly Hoa Beach [Master's Thesis]. Lund University: Lund, Sweden. p. 70. Available from: https://lup.lub.lu.se/luur/download?fileOId=1333108&func=downloadFile&recordOId=1333107

[26] Fang, G., Kwok, Y.-K., Yu, K., et al., 1999. Numerical simulation of principal tidal constituents in the South China Sea, Gulf of Tonkin and Gulf of Thailand. Continental Shelf Research. 19(7), 845–869. DOI: https://doi.org/10.1016/S0278-4343(99)00002-3

[27] Quynh, L.T.P., Garnier, J., Gilles, B., et al., 2007. The changing flow regime and sediment load of the Red River, Vietnam. Journal of Hydrology. 334(1–2), 199–214. DOI: https://doi.org/10.1016/j.jhydrol.2006.10.020

[28] Copernicus Marine Environment Monitoring Service (CMEMS), 2023. Global Ocean Waves Reanalysis. Available from: https://doi.org/10.48670/moi-00022 (cited 1 December 2025).

[29] Mase, H., 2001. Multi-directional random wave transformation model based on energy balance equation. Coastal Engineering Journal. 43(4), 317–337. DOI: https://doi.org/10.1142/S0578563401000396

[30] Law Chune, S., Aouf, L., Dalphinet, A., et al., 2020. WAVERYS: A CMEMS global wave reanalysis during the altimetry period. In Proceedings of EGU General Assembly 2020, Online, 4–8 May 2020. DOI: https://doi.org/10.5194/egusphere-egu2020-7062

[31] Reguero, B.G., Menéndez, M., Méndez, F.J., et al., 2012. A Global Ocean Wave (GOW) calibrated reanalysis from 1948 onwards. Coastal Engineering. 65, 38–55. DOI: https://doi.org/10.1016/j.coastaleng.2012.03.003

[32] Häglund, M., Svensson, P., 2002. Coastal erosion at Hai Hau Beach in the Red River Delta, Vietnam [Master's Thesis]. Lund University: Lund, Sweden. p. 80. Available from: http://lup.lub.lu.se/student-papers/record/1333117

[33] U.S. Army Corps of Engineers (USACE), 1984. Shore Protection Manual, Volume 1. Coastal Engineering Research Center, Department of the Army Waterways Experiment Station, Corps of Engineers: Washington, DC, USA. Available from: https://usace.contentdm.oclc.org/digital/collection/p16021coll11/id/1934/

[34] Bijker, E.W., 1971. Longshore transport computations. Journal of the Waterways, Harbors and Coastal Engineering Division. 97(4), 687–701. DOI: https://doi.org/10.1061/AWHCAR.0000122

[35] Wijdeven, B., 2002. Coastal Erosion on a Densely Populated Delta Coast: The Interactions between Man and Nature—A Case Study of Nam Dinh Province, Red River Delta, Vietnam [Master's Thesis]. Delft University of Technology: Delft, Netherlands. p. 163. Available from: https://resolver.tudelft.nl/uuid:c844fe54-2421-46d4-a26b-3352e5bcdc61

[36] Donnelly, C., Hung, N.M., Larson, M., et al., 2004. One-line modelling of complex beach conditions: An application to coastal erosion at Hai Hau Beach, Vietnam. In Proceedings of the 29th International Conference on Coastal Engineering, Ha Long, Vietnam, 19–24 September 2004; pp. 2449–2461. DOI: https://doi.org/10.1142/9789812701916_0197

[37] Hanson, H., Kraus, N.C., 1989. GENESIS: Generalized Model for Simulating Shoreline Change, Report 1—Technical Reference. U.S. Army Corps of Engineers: Washington, DC, USA. Available from: https://dn790006.ca.archive.org/0/items/genesisgeneraliz00hans/genesisgeneraliz00hans.pdf

[38] Birkemeier, W.A., 1985. Field data on seaward limit of profile change. Journal of Waterway, Port, Coastal, and Ocean Engineering. 111(3), 598–602. DOI: https://doi.org/10.1061/(ASCE)0733-950X(1985)111:3(598)

[39] Valiente, N.G., Masselink, G., Scott, T., et al., 2019. Role of waves and tides on depth of closure and potential for headland bypassing. Marine Geology. 407, 60–75. DOI: https://doi.org/10.1016/j.margeo.2018.10.009

[40] Quang, N.H., Viet, T.Q., 2023. Long-term analysis of sediment load changes in the Red River system (Vietnam) due to dam-reservoirs. Journal of Hydro-environment Research. 51, 48–66. DOI: https://doi.org/10.1016/j.jher.2023.10.002

[41] Cong, M.V., 2004. Safety Assessment of Sea Dikes in Vietnam: A Case Study in Namdinh Province [Master's Thesis]. UNESCO-IHE Institute for Water Education: Delft, The Netherlands. Available from: https://resolver.tudelft.nl/uuid:1048220e-d274-4abe-b2c0-fa324a15eae9

[42] Cong, V.M., Stive, M.J.F., Van Gelder, P.H.A.J.M.,

et al., 2009. Coastal Protection Strategies for the Red River Delta. Journal of Coastal Research. 2009(251), 105–116. DOI: https://doi.org/10.2112/07-0888.1

[43] Hoan, L.X., Hanson, H., Larson, M., et al., 2011. Modeling regional sediment transport and shoreline response in the vicinity of tidal inlets on the Long Island coast, United States. Coastal Engineering. 58(6), 554–561. DOI: https://doi.org/10.1016/j.coastaleng.2011.03.003

[44] Angnuureng, D.B., Charuka, B., Almar, R., et al., 2025. Challenges and lessons learned from global coastal erosion protection strategies. iScience. 28(4), 112055. DOI: https://doi.org/10.1016/j.isci.2025.112055

[45] Angnuureng, B.D., Adade, R., Chuku, E.O., et al., 2023. Effects of coastal protection structures in controlling erosion and livelihoods. Heliyon. 9(10), e20633. DOI: https://doi.org/10.1016/j.heliyon.2023.e20633

[46] Saengsupavanich, C., Rif'atin, H.Q., Magdalena, I., et al., 2024. A systematic review of jetty-induced downdrift coastal erosion management. Regional Studies in Marine Science. 74, 103523. DOI: https://doi.org/10.1016/j.rsma.2024.103523

[47] Wang, Y.-H., Wang, Y.-H., Deng, A.-J., et al., 2022. Emerging downdrift erosion by twin long-range jetties on an open mesotidal muddy coast, China. Journal of Marine Science and Engineering. 10(5), 570. DOI: https://doi.org/10.3390/jmse10050570

[48] van Maren, D.S., Alonso, A.C., Engels, A., et al., 2023. Adaptation timescales of estuarine systems to human interventions. Frontiers in Earth Science. 11, 1111530. DOI: https://doi.org/10.3389/feart.2023.1111530

[49] Carvalho, R.C., Woodroffe, C.D., 2023. Coastal compartments: The role of sediment supply and morphodynamics in a beach management context. Journal of Coastal Conservation. 27, 58. DOI: https://doi.org/10.1007/s11852-023-00984-6

[50] Marino, M., Nasca, S., Alkharoubi, A.I., et al., 2025. Efficacy of Nature-based Solutions for coastal protection under a changing climate: A modelling approach. Coastal Engineering. 198, 104700. DOI: https://doi.org/10.1016/j.coastaleng.2025.104700

[51] Huynh, L.T.M., Su, J., Wang, Q., et al., 2024. Meta-analysis indicates better climate adaptation and mitigation performance of hybrid engineering-natural coastal defence measures. Nature Communications. 15, 2870. DOI: https://doi.org/10.1038/s41467-024-46970-w